International Journal of Thin Films Science and Technology

http://dx.doi.org/10.18576/ijtfst/110310

Enhancement of Structural, Optical and Bumpy Surface Effect of Cu_2O Thin Films Through Sn Doping by Modified SILAR Technique

A. Vasuhi [1], *K. Dhanabalan* [2,*], *A. T. Ravichandran* [3], *R. Chandramohan* [4] *and Srinivas Mantha* [5]

[1]Department of Physics, H.H. The Rajah's College (Autonomous) (Affiliated to Bharathidasan University), Pudukkottai, Tamilnadu, India- 622 001
[2]Post Graduate and Research Department of Physics, J.J. College of Arts and Science (Autonomous) (Affiliated to Bharathidasan University), Pudukkottai, Tamilnadu, India -622 422
[3]Post Graduate and Research Department of Physics, National College (Autonomous) (Affiliated to Bharathidasan University), Tiruchirappalli, Tamilnadu, India- 620 001
[4]PG Department of Physical Sciences, Vidhyaa Giri College of Arts and Science, Puduvayal - 630108, India
[5]Department of Electronics and Communication Engineering, SAGE University, Bhopal, 462022, India

Received: 2 Jun. 2022, Revised: 12 Jul. 2022, Accepted: 21 Aug. 2022.
Published online: 1Sep. 2022.

Abstract: Undoped and Sn doped $Cu_{2-x}Sn_xO$ (x = 0, 5.0, 10.0, 15.0 and 20.0) thin films have been deposited into glass substrates by hire a fee powerful method of M-SILAR (Modified-Successive Ionic Layer Adsorption and Reaction). The Sn doping level in the starting solution become numerous from 0 to 20.0 mol.% in steps of 5.0 mol.%. The deposited films were characterized for their structural, optical, morphological and topography properties with respective instrumentation. X-ray diffraction (XRD) evaluation found out the orientation of crystalline increase of $Cu_{2-x}Sn_xO$ films, and all the films showcase single crystalline. The preferential orientation was retained in favor of (111) plane even at the highest doping level. The presence of copper in the films turned into showed by way of energy dispersive X-ray spectrometer. Average optical transmittance (UV-vis-NIR and Photoluminescence (PL)) are varied with effect of doping concentration. The stretching vibrations of Cu-O, Sn-O and O-Cu-O have been showed by using Fourier transform infrared spectroscopy (FTIR). The morphological observe has been achieved by using a Field emission scanning electron microscopy (FE-SEM) has display as decrease the particle length with increase of doping concentration. From High resolution transition electron microscopy (HR-TEM) the crystalline growth of each line are excellent within the Sn doping of 10.0 mol.%. The atomic force microscopy method changed into employed to investigate the roughness of the films and the bumpy surface revealed at 10.0 mol.% of Sn doping level.

Keywords: Low Cost, Cu2O Thin Film, Heavily Sn-Doped, FE-SEM, HR-TEM, AFM.

1 Introduction

Metal oxide are an critical magnificence of substances from both medical and technological perspectives they gift thrilling possibilities for research. Thin films are specifically appealing as a result of their relevance in devices, and also for the ability to pursue surface-belongings family members research the usage of controlled microstructures. They are the distinguished substances gambling important function in digital device and also attractive substances for solar power conversion [1] and photo catalytic activity programs [2]. Among diverse metal oxide materials, the copper oxides are promising semiconductor substances for a extensive variety of optoelctronic devices to their semi conductivity with a band hole of ≈ 2.1 eV respectively [3]. Recently, steel oxide materials are relevant in all fields, of their pure and doping thin films. The conductivity of the Cuprous oxide (Cu_2O) film will increase, when the doping is a very vital technique to growth the conductivity of the film by increasing the variety of intermediate strength tiers created in the energy band gap location [4]. Cuprous oxide behaves because the figure compound in many p-type semiconductor for obvious undertaking oxides (TCOs) materials (TCOs : Al, Mn, Fe, Li, Ni, Ti, Zn, Co, and so on.,….) [5-9]. The Sn-doped Cu_2O delafossite thin film ion be used in layer-portions and serves as the important

*Corresponding author E-mail: dhana_pgp@rediffmail.com

transition elements. Because, Sn is similar ionic radius to Cu^{2+} (Cu^{2+} ionic radius is 0.73 Å and Sn^{2+} ionic radius is 0.69 Å) which could alternative without problems for Sn^{2+}, resulting in little lattice distortion. Cuprous oxide is a appropriate candidate for the Bose-Einstein condensation due to its better binding electricity. The material can be utilized in a huge levels software which includes solar power[10,11], photograph catalyst[12], fuel sensors[3], dilute magnetic semiconductor[14], lithium-ion batteries[15] and obvious conductors[16]. Cuprous-oxide nanostructured thin films have been deposited via numerous techniques, like sputtering[17], pulsed lased deposition[18], chemical vapour deposition[19], spray pyrolysis[20], plasma evaporation[21], electro chemical deposition [22], chemical bathtub deposition[23], one step hydro thermal [24], magnetic reactive sputtering[25], epitaxial boom[26] and successive ionic layer adsorption and response (SILAR) [27]. Among numerous approach, the thin film's deposition process, the SILAR approach has greater blessings, which include low fee effective approach, low temperature blending of composition at the molar ratio, non-toxic, and big vicinity deposition with a unique stoichiometry.

2 Materials and Methods

Cuprous oxide (Cu_2O) thin films have been deposited onto glass substrates using a SILAR method. The deposition parameters employed within the present observe is offered in Table 1.

Table 1: Deposition Parameters.

Deposition parameters employed in this study	
Cationic precursor (M)	Copper Sulfate Pentahydrate (0.1 M) + Sodium Thiosulfate (0.1 M)
Anionic precursor (M)	Sodium Hydroxide (1 M)
Dopant precursor	Tin Sulphate ($SnSO_4$) (0, 5.0, 10.0, 15.0 &20.0 mol. %)
Temperature of cationic solution	Room Temperature
Temperature anionic solution	70°C
Dipping time in cationic solution	20 sec
Dipping time in cationic solution	20 sec
Number of dipping cycles	30

The substrates have been pre-cleaned ultrasonically with natural solvents and deionized water to remove the contaminations if any on the surface. These cleaned substrates were immersed in NaOH solution for 20 sec so that OH- ions from NaOH solution are adhered to the surface of the substrate. Then, the substrate became immersed for 20 sec in the copper thiosulfate complex solution which changed into organized by dissolving a suitable amount of cationic precursor material in deionized water. These substrates have been then immersed in deionized water (maintained at room temperature) for 10 sec to dispose of the loosely bound ions. These three immersions combinedly represent one cycle of a deposition. This cycle of immersions is repeated until the specified thickness is reached. The Sn doped Cu_2O thin film were prepared through adding suitable quantity of Tin Sulphate ($SnSO_4$) (Stannous Sulphate) salt in the cationic solution. A schematic representation of the SILAR method is shown in Fig. 1.

The process was repeated as much as 30 cycles to obtain good the quality of undoped and Sn - doped Cu_2O thin films. Fig. 2 shows the deposition of thin films onto glass substrates. The deposited films were characterized significantly using the following gadgets. The deposited film have been characterized extensively the use of the subsequent instruments. Average thickness may be determined via understanding the average step height (ASH) at any region in the experiment region the use of the surface profiler dektak150. X-ray diffraction sample of the films changed into acquired using X'pert PRO (PANalytical) diffractometer with CuKα radiation (k = 0.15405 nm). The formation of the copper oxide became similarly confirmed through FTIR Spectroscopy (Model: Spectrum RXI, Make: Perkin Elmer). To determine the band gap energy of the films, the optical-transmission changed into recorded the usage of Perkin Elmer Lambda 35 spectrophotometer. Photoluminescence (PL) spectra have been studied using a Spectroflurometer (JobinYvon_FLUROLOG-FL3-eleven). The morphological analysis of the films was performed using Hitachi (S-3000H) field emission scanning electron microscope. HR-TEM images and electron diffraction patterns for the film layers had been measured the use of the JEOL JEM 2100, 2 hundred KV running voltage. The Atomic pressure microscope (AFM) studies were carried out the use of the device of (Veeco-di CP II). The outcomes are mentioned below.

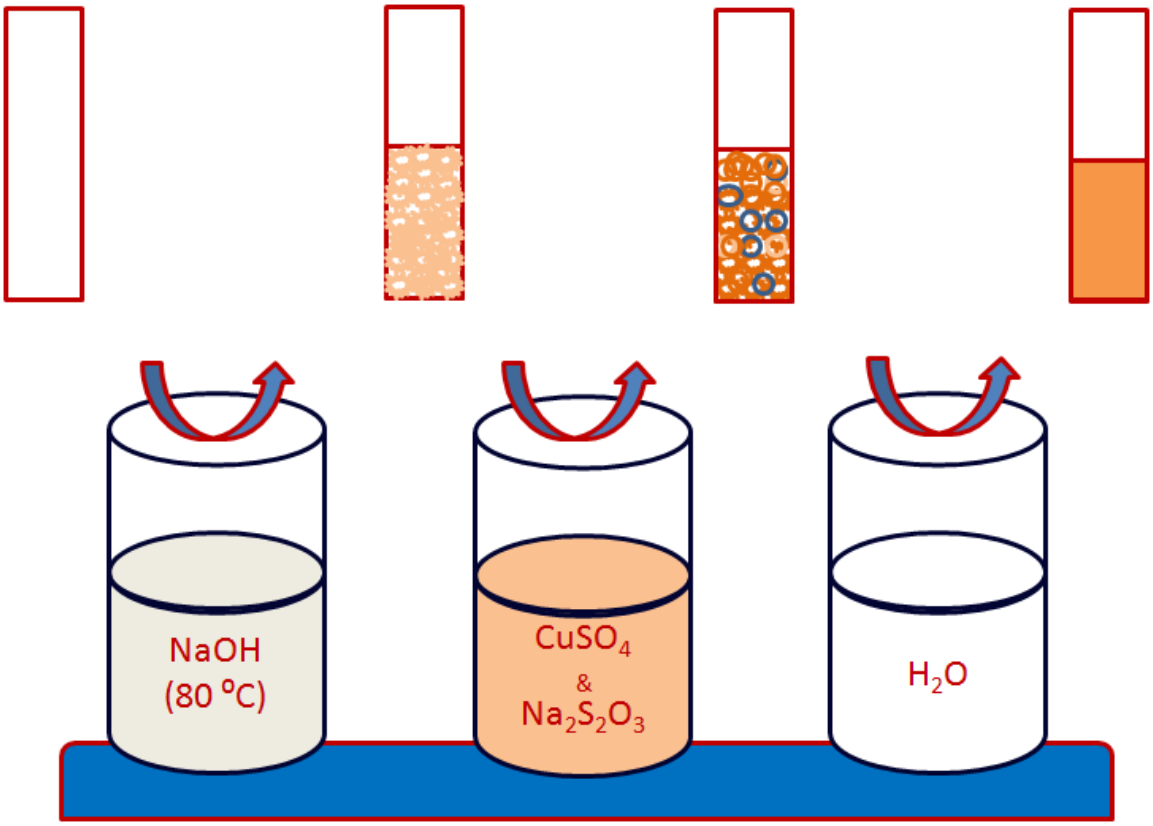

Fig. 1: Schematic diagram of the SILAR technique.

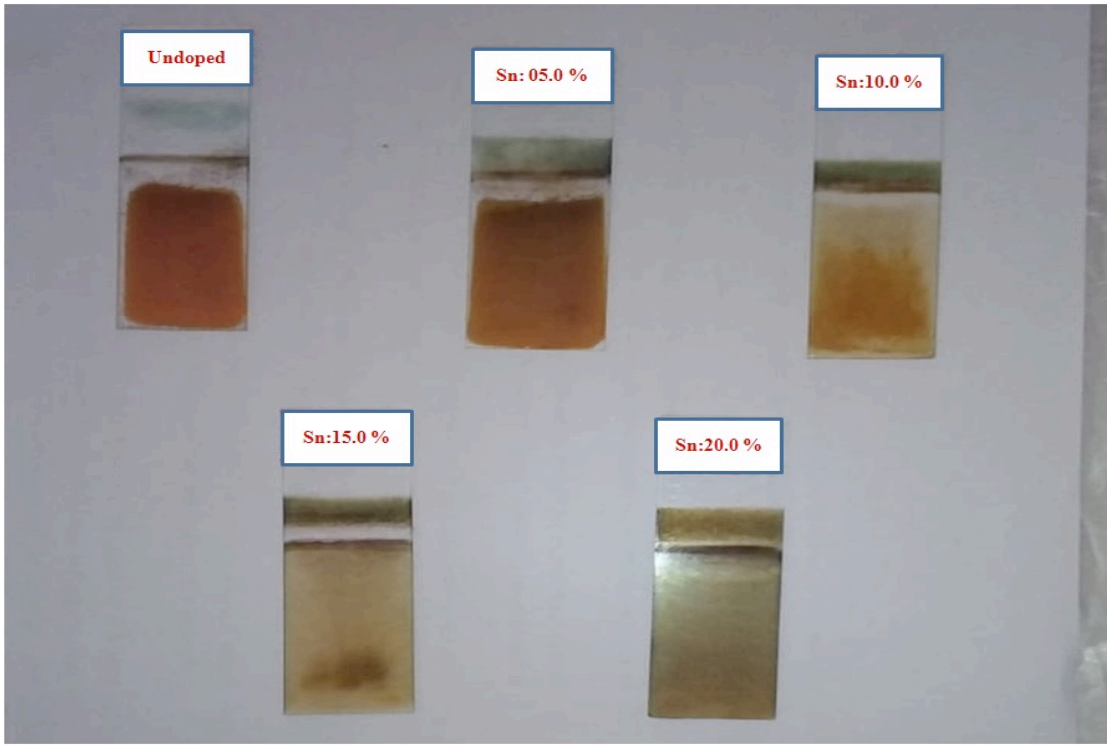

Fig. 2: Deposited thin films onto a glass substrate.

3 Results and Discussion

3.1 Thin film thickness measurement:

The measurement of thin film thickness is incredibly important for many applications like semiconductor devices, displays for various goods and optical manufactured goods coatings. Two measurement has been done in all sample at different places. Table 2 show the thickness measurement of undoped and Sn doped thin films. In Fig. 3 shows the graph of undoped and Sn doped cuprous oxide Vs thickness of the films. However, the thickness of the film increase with increase of Sn 5.0 mol.%. But, Further increases Sn doping level up to 10.0 mol.%, unfortunately the thickness of the film decreases. Again increases the Sn concentration (10.0, 15.0 and 20.0 mol.%) the thickness of film layer increases linearly.

Fig. 4. shows the X-ray diffraction patterns of glass substrate, undoped and Sn doped Cu_2O thin films. The XRD patterns exposed that all the characterized films are single crystallines in nature, except the one deposited with 20.0 mol.% of Sn which exhibits an amorphous state. All the film exhibit the cubic structure of cuprous oxide crystal structure (JCPDS Card No: 05-0667). No other secondary peaks correspond to secondary phases are detect. It's indicating the purity of the arranged films or the presence of undetected level of pollution in the prepared Cu_2O thin films. In the case of undoped film, the diffraction line corresponds to (111) orientation plane of Cu_2O. The intensity of (111) peak increases with increase of Sn doping concentration. However, the intensity of (111) peak drastically increased (nearly double time compared to undoped film), when Sn doped with Cu_2O up to 10.0 mol.%. The low intensity of the diffraction peak in the case of undoped cuprous oxide (Cu_2O) film may be

Table 2: Structural and optical parameters of Sn doped Cu2O thin films.

S.No.	Sn Doping level (mol.%)	Crystallities Size D (nm)	Lattice Parameters (a) nm	Thickness of the films (μm)	Dislocation density(δ) (lines/m^2) X10^{-15}	Micro strain (ε) X10^{-3}	Optical energy band gap (eV)
1.	0	52.07	4.3022	0.79	1.8507	1.4912	1.70
2.	05.0	46.27	4.2893	0.58	1.6274	1.8228	1.73
3.	10.0	36.49	4.2942	0.52	1.3181	2.3453	2.18
4.	15.0	28.34	4.2613	1.07	0.9683	2.6797	2.10
5.	20.0	23.24	4.2137	1.26	0.4042	3.2024	1.80

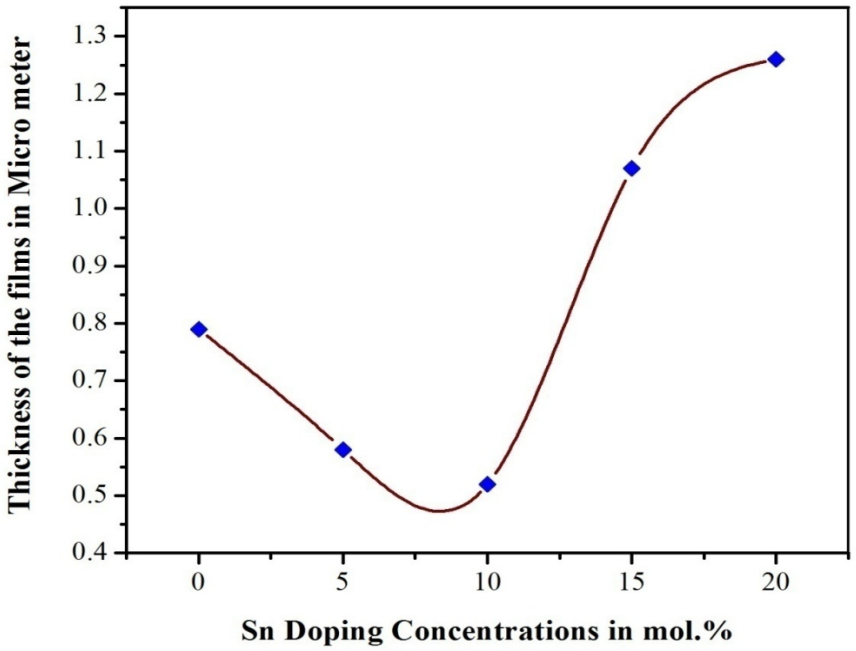

Fig. 3: Undoped and Sn doped cuprous oxide thin films Vs thickness of the film.

ascribed to the presence of many Cu and O vacancy in the Cu_2O lattice. But, when Sn^{2+} is doped with the Cu_2O, the Cu^{2+} and O^- is may be settled at the Cu and O^{2-} vacancies. The compensation of vacancies improving the periodic alignment of crystal lattice. However, at higher doping level (15.0 and 20.0 mol.%), the interstitial amalgamation of excess Sn^{2+} ions may cause worsening in the crystalline quality of the films. The maximum doping of Sn (20.0 mol.%) the spectra show practically an amorphous nature of the Cu_2O film (very feeble diffraction peak exhibit). It may be, interstitial incorporation of excess of Sn^{2+} (nearly three times compared to the deposition of 5.0 mol.% film). This suggest that Sn ions stay behind mainly in solution to bond with other atom, in particular hydrogen only few Sn ions are included in the form of film

[28]. The particles are stream line of amorphous nature. The presence of Sn in the Cu_2O sample is inveterate by EDAX spectra shown in Fig. 5. The chemical composition of Sn doped Cu_2O film with 5.0 mol.% is shown in the inset table of Fig. 5. Average crystalline

quality of the films were considered using the Debye-Scherrer's formula [29].

$$D=\frac{k\lambda}{\beta\cos\theta} \quad \text{(1)}$$

Where D- is the crystallite size, k- is the shape factor (k = 0.9), λ – is the wavelength of x-rays, β- is the full-width half maximum (FWHM).

The lattice parameter 'a' of the cubic system of Cu_2O film and dislocation density (δ)and micro strain (ε) are calculated using the formula [30] and the values are given table.2.

$$\frac{1}{d^2}=\frac{h^2+k^2+l^2}{a^2} \quad \text{(2)}$$

$$\delta=\frac{1}{D^2} \quad \text{(3)}$$

$$\varepsilon=\frac{\beta\cos\theta}{4} \quad \text{(4)}$$

3.2 X-Ray diffraction analysis:

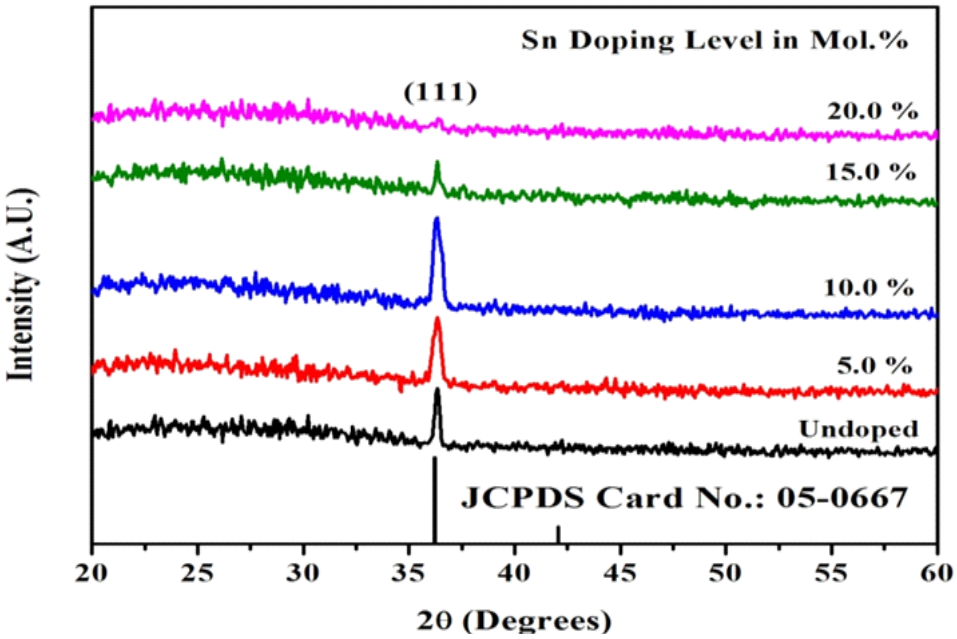

Fig. 4: X-ray diffraction pattern of cuprous oxide thin films deposited by SILAR method at different concentration of Sn.

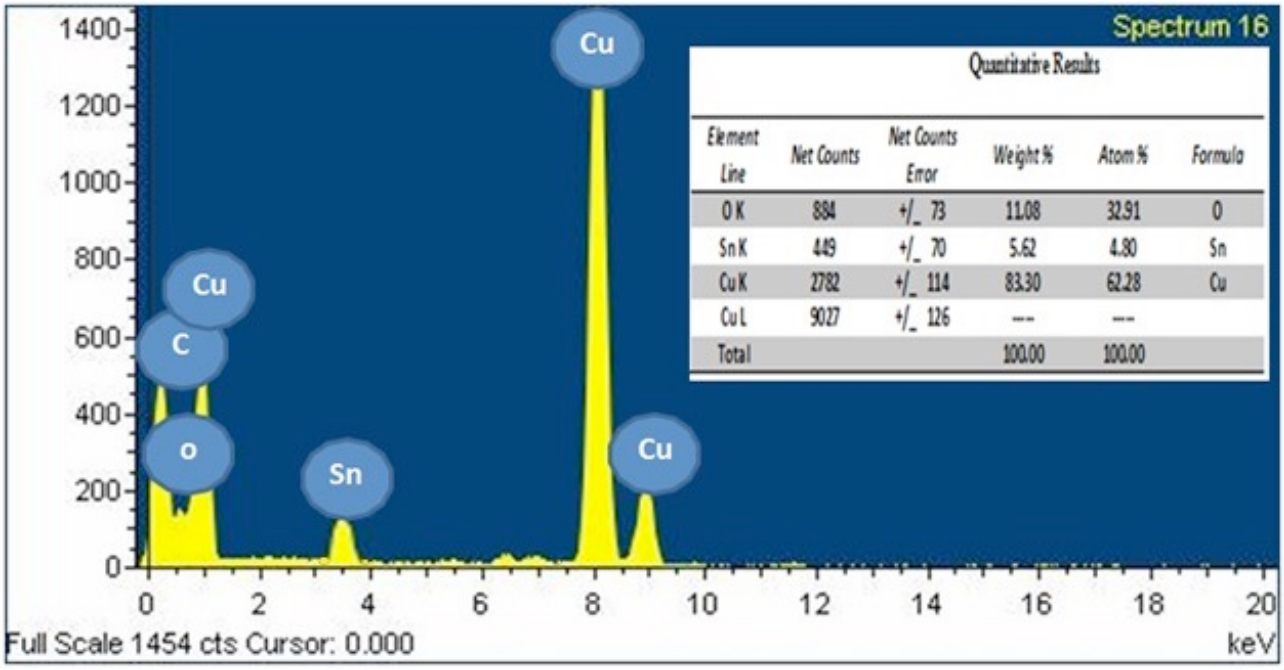

Fig. 5: EDAX Spectrum of Sn doped thin film at 10.0 mol%.

3.3 Optical Properties:

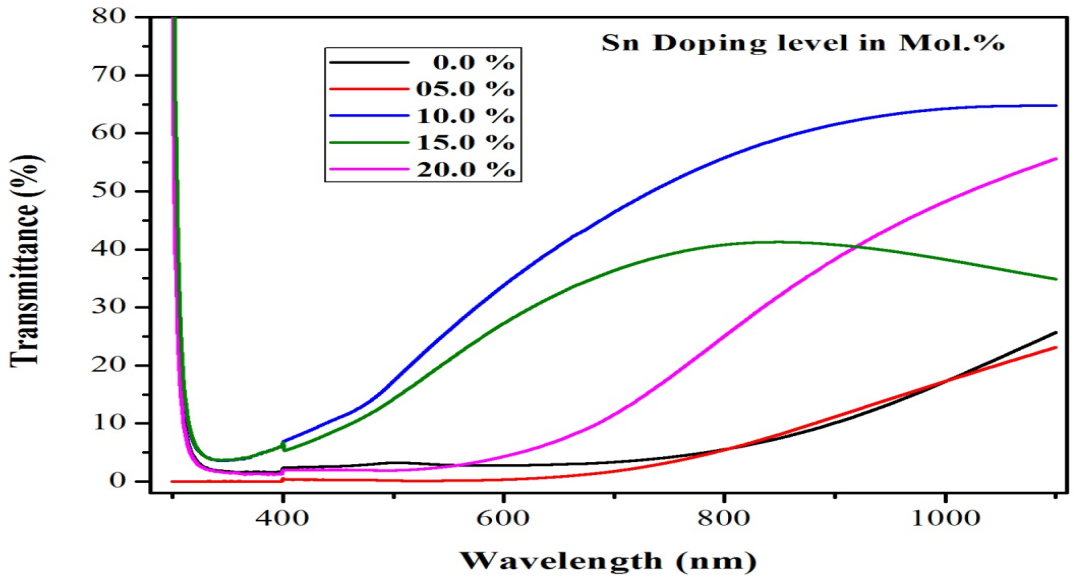

Fig. 6: UV-vis-NIR transmittance spectrum of undoped and Sn doped Cu_2O thin films.

Fig. 6 shows the transition spectrum of undoped and Sn doped cuprous oxide thin films (Sn : 0, 5.0,10.0,15.0 and 20.0 mol.%) and the range between wavelength 300 to 1100 nm. The Cut off wavelength of the film are revealed nearly 400 nm. The average optical transmittance in the visible region is 30 % for the undoped Cu_2O thin film. The transmittance of the film are gradually increased with increase of Sn doping attentiveness up to 10.0 mol.% (≈ 70 %). Further, increase the Sn doping concentration the transmittance of the film decreases. The doping of Sn (10.0 mol.%), the transmittance of the film is very high. The transmittance of the film varied, it may be due to the dissimilarity in the crystalline and grain sizes owing to doping. The high transmittance in the visible region, it's useful for aesthetic window glass materials. It's clearly seen that the crystalline size increases with increase of doping level as shown in Table 2. Fig. 7 shows the optical absorbance spectra of the films at room temperature from the range of 300- 1100 nm. The large area of absorptions in the visible region used for solar cell applications The essential absorption can be used to establish the band-gap of the films as shown in Fig. 8. The optical band gap of the films are predictable using from the Tauc's plot relation[31] of absorption coefficient (α) and the photon energy (hν) as

$$(\alpha h\nu)^2 = A\,(h\nu - Eg)$$

Where A and Eg are the constant and optical band gaps correspondingly. The Eg can be determine by extrapolation of linear portion of the curve to the hν axis. The energy band gap (Eg) values are increases with increase of Sn doping level upto 10.0 mol.%. Further, decreases the energy band gap value with increases of Sn doping level. The energy band gap value varied from 1.70 to 2.18 eV. It proves the crystalline enhancement of the film at the Sn doping level of 10.0 mol%.

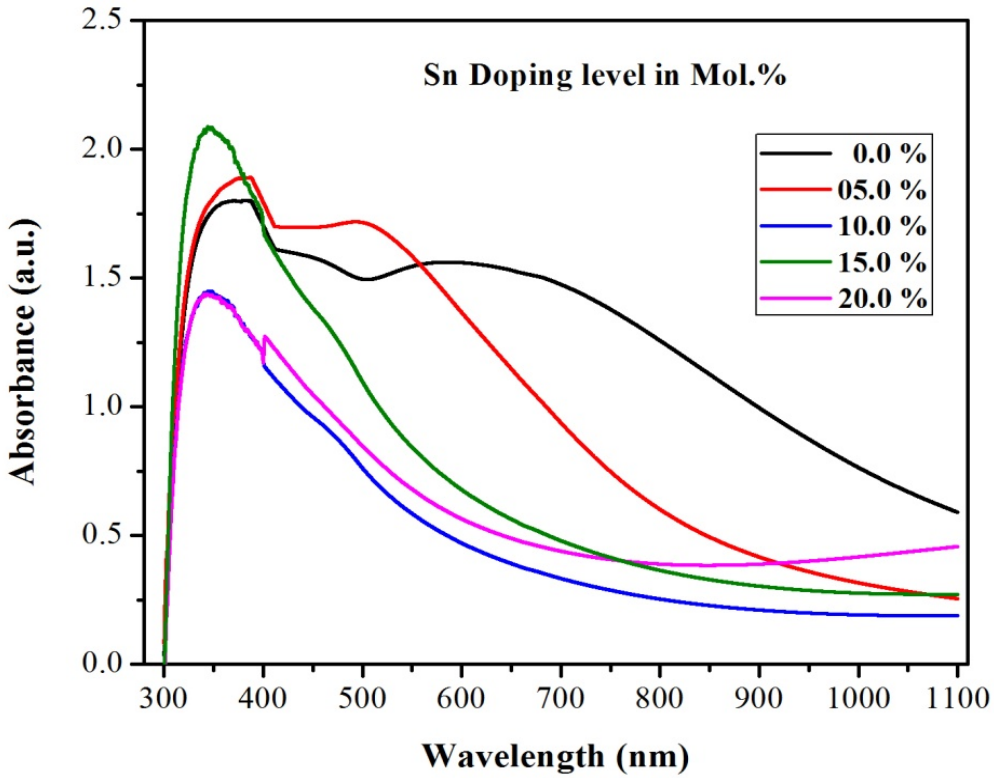

Fig. 7: UV-vis-NIR absorbance spectrum of undoped and Sn doped Cu_2O thin films.

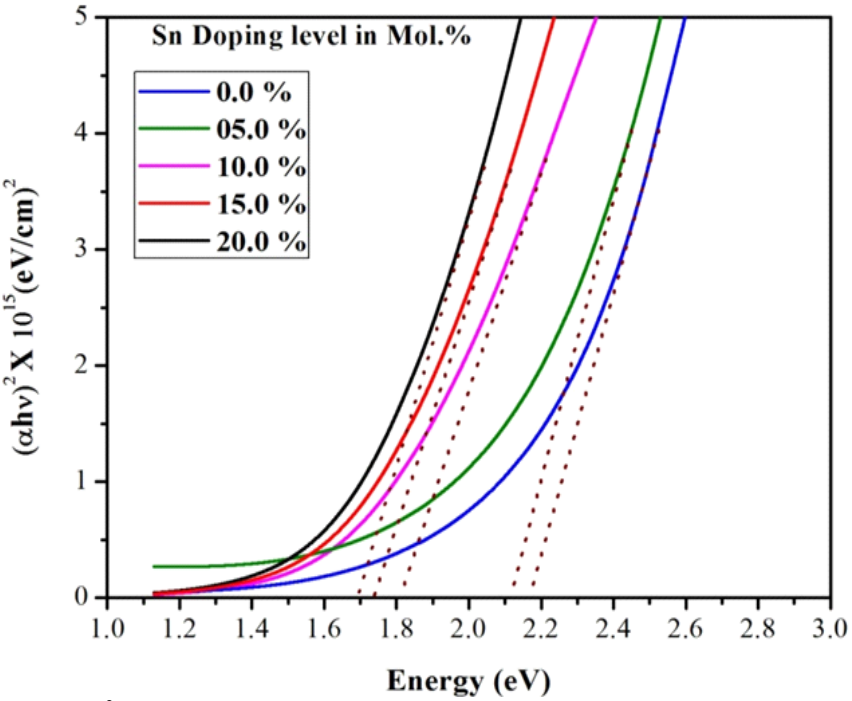

Fig. 8: The variation of $(\alpha h\nu)^2 Vs(h\nu)$ for undoped and Sn doped Cu_2O thin films at different Sn concentration.

3.4 Fourier Transform Infrared Spectroscopy:

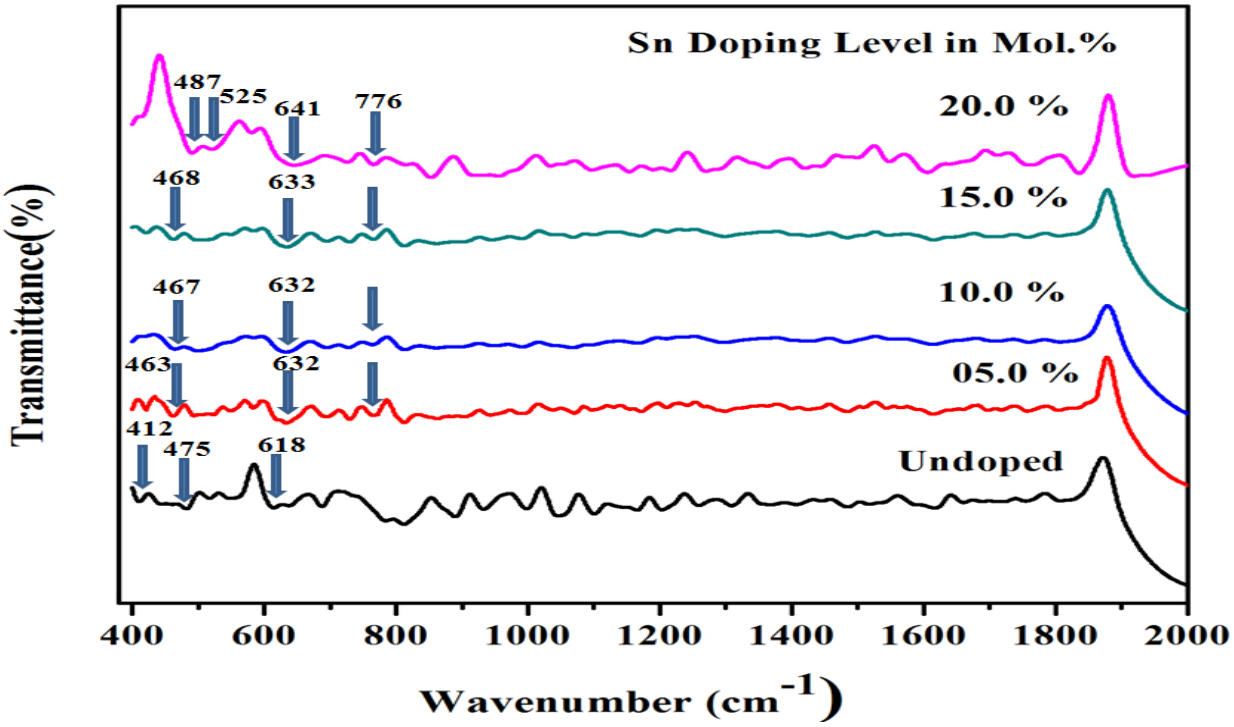

Fig. 9: FTIR spectrum of undoped and Sn doped Cu_2O thin films at different Sn concentration.

Fig. 9 shows the Fourier transform infrared (FTIR) spectrum of undoped and Sn doped Cu_2O thin films. The band spectrum has been recorded in the region between 400 to 2000 wave number (cm^{-1}). The vibrational frequencies of different chemical bonds in the films can be assign the FTIR spectra regarding the peaks absorption positions. The FTIR spectrum of cuprous oxide (Cu_2O) presents 412 and 475 cm^{-1} for the undoped film. Further, increase the Sn doping concentration (5.0, 10.0, 15.0 and 20.0 mol.%) the more absorption peaks are revealed at 463, 467, 468, 487 and 525 cm^{-1} correspondingly. These absorption peaks corresponds to the stretching vibrations of Cu-O in the cuprous oxide thin films [32]. The peak at 618 cm^{-1} is attributed and it's able to evidence of the formation of Cu_2O [33]. The peak at 618 cm^{-1} is shifted towards the higher wave number (cm^{-1}) such as the peaks at 632, 633 and 641 cm-1 whenthe Sn doping concentrations equivalent to the stretching vibrations of cubic system. The peaks at 776 cm^{-1} are ascribed to the formation of Sn-O stretching vibrations[34].

Fig.10 shows body temperature photoluminescence (PL) spectra of undoped and Sn doped Cu_2O thin films with different concentrate of doping. The photoluminescence spectra are frequently used to reveal the competition between electron-hole separation to electron-hole recombination. All the films exhibit the peak at 361 nm (Violet), 495 nm (Green-I) and 520 nm (Green- II). The near band emission (NBE) peaks are appear nearly at 520 nm [35]. All the Sn doped peaks are shifted towards the lower wavelength compared to undoped film spectra. It is revealed to the Moss-Bursten effect [36,37]. It can be ascribed to the dissimilarity of the optical band gap of the material.

3.5 Photoluminescence:

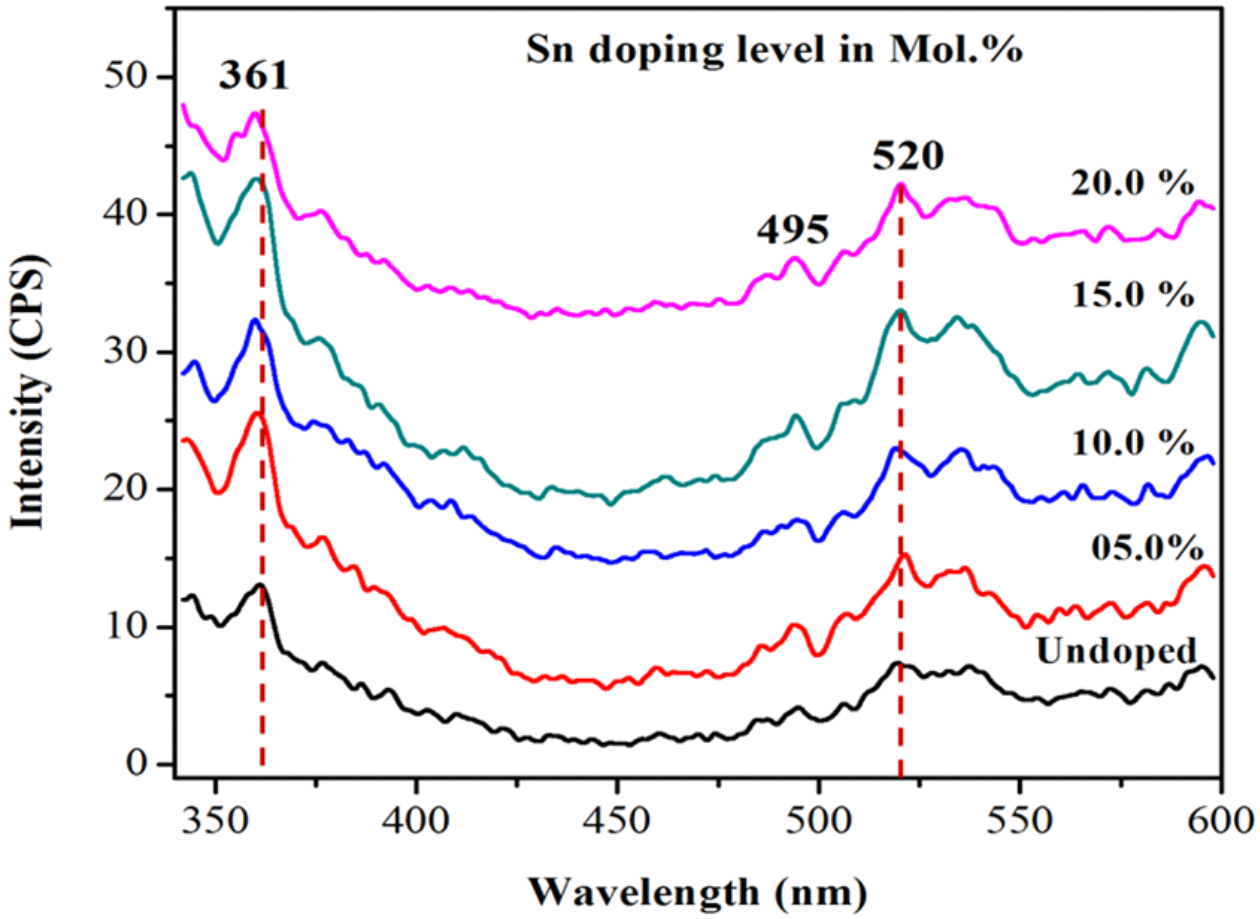

Fig. 10: Photoluminescence spectrum of undoped and Sn doped Cu_2O thin films at different Sn concentration.

3.6 Surface Morphology

The surface morphology of the undoped and Sn doped films are analyzed using field emission scanning electron microscope (FE-SEM) images. The image Fig.11 clearly depict to the grain size increase gradually the doping level increases. In the case of undoped film, huge number of rod-like structure appeared through different size of length and breath. We can see (left top corner) numerous small nano-rods are agglomerated, due to Van-der walls force [38] as shown in Fig.(11.(a)). Fig. (11.(b)) shows, assembled nano-rod like structure without separation of individual formation. Here, the doping concentrations are affected the surface properties of the film. Further, increasing doping concentration (10.0 mol.%), the surface of the film depict clearly nano-rods and 3D flower-like structure. The nano-rods are perfectly indicated with different length as shown in Fig. (11.(c)). In the case of Sn doped Cu_2O (Sn : 15.0 mol.%) all nano-rods and flower-like structure disappeared and appear large number of grain with different size as shown in Fig. (11.(d)). The maximum doping of Sn concentration (Sn : 20.0 mol.%) the surface morphology appear amorphous nature as shown in Fig. (11.(e)). The result is correlated with XRD results.

3.7 TEM and HR-TEM:

The size and morphology of the nano particles and perfectly arrangement of crystal orientation grow of the films were further investigated using TEM and HRTEM analysis. Fig. 12 shows the TEM, HTEM and SEAD patterns are analysis for undoped and Sn doped cuprous oxide (Cu_2O) thin films for 0.0, 5.0,10.0, 15.0 and 20.0 mol.% respectively. The undoped TEM image are revealed a large cloud like particle. That means, the obtained cuprous oxide nano-grins are single crystalline as shown in Fig. (12.(a)). Now adding the Sn doping concentrations like 5.0, 10.0, 15.0 and 20.0 mol.% the surface of the film affected. Moreover, the concentration of Sn doping are exaggerated the morphology and phase be in charge of cuprous oxide nano structures during the deposition reaction process. No cuprous oxide polycrystalline can be obtained but single crystalline. A typical TEM image of an isolated undoped and Sn doped Cu_2O nanoellipsoid in Fig. 12 shows a uneven surface, representing that the structure assembled from minute nano particles. The HR-TEM images are taken from central surface of an individual undoed and Sn doped Cu_2O nanoellipsoid as illustrated, and the exaggeration of

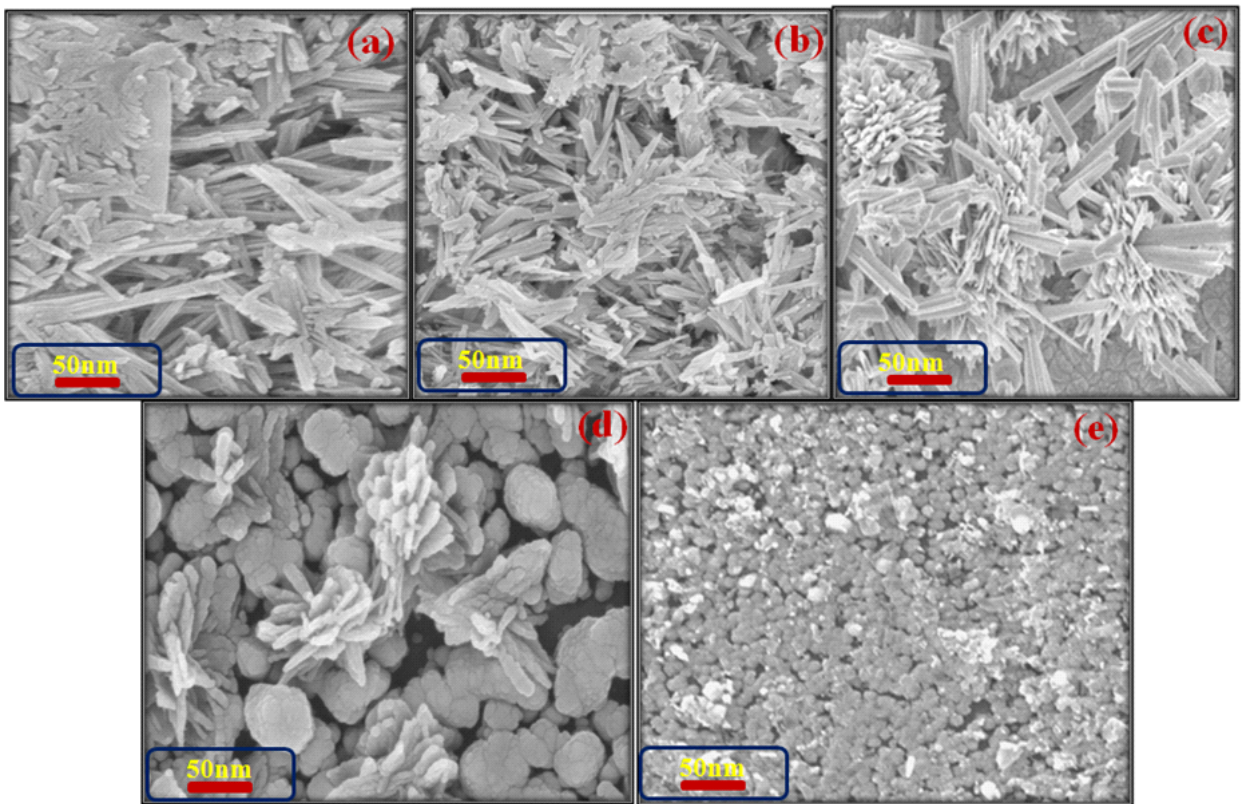

Fig. 11: FESEM images of undoped and Sn doped Cu_2O thin films at different Sn concentration.

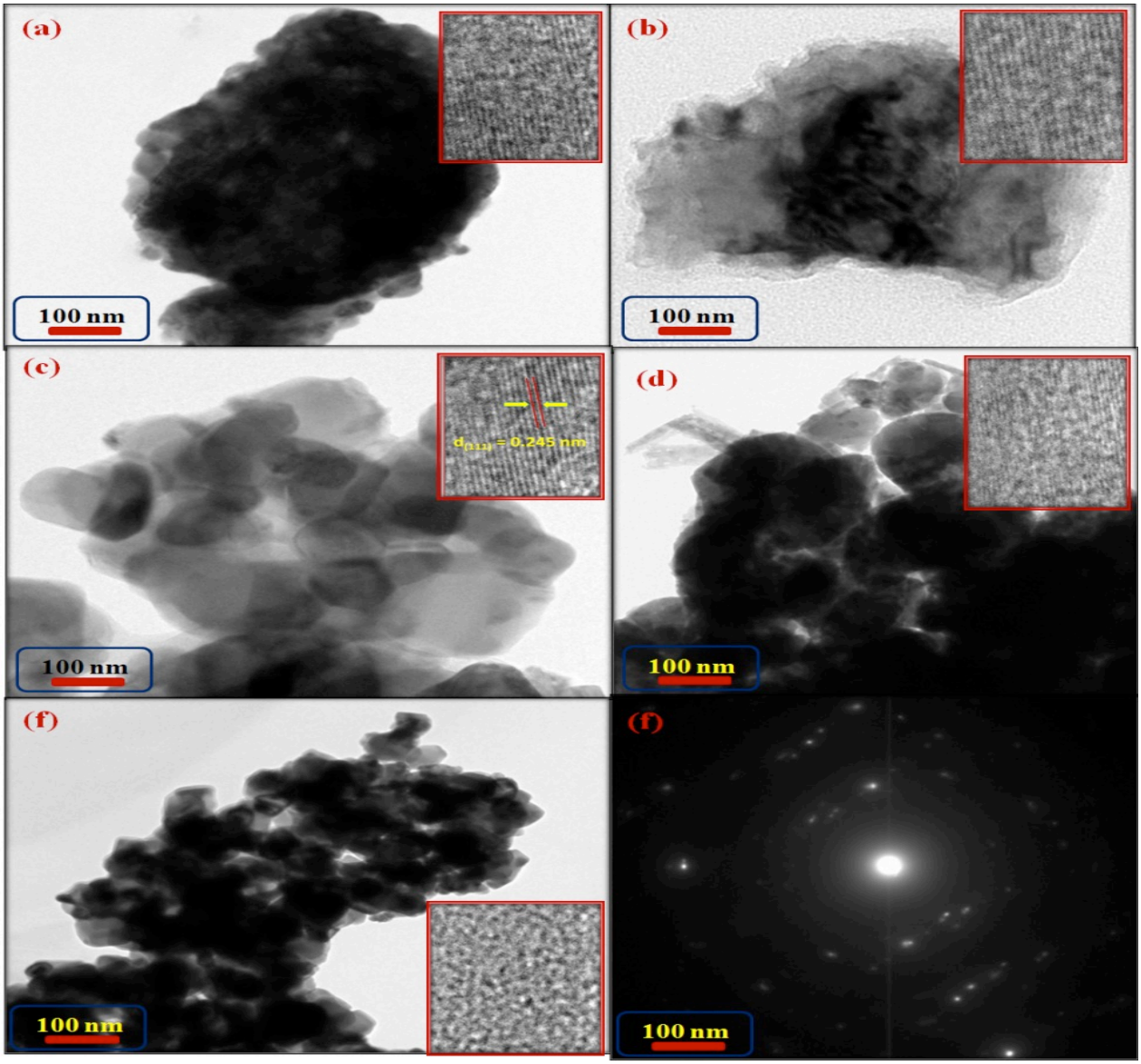

Fig. 12: TEM and HRTEM (inset) images of undoped and Sn doped Cu_2O thin films at different Sn concentration.

HR-TEM are insets in the top right corner of TEM images as shown in Fig. 12. The enlargement of HR-TEM indicate, the orientation of crystalline line is clearly not appear except the Sn doped with 1.0 mol % of cuprous oxide film. Here found that both fringe spacing are 0.245 nm which equivalent to the (111) plane of cubic cuprous oxide. The fringe spacing are clearly depict in the Sn doped (10.0 mol.%) Cu_2O film. The result implies that the subunits oriented bring together with each other. Fig. (12.(f)) shows the SEAD pattern of Sn doped Cu_2O thin film (Sn doped with 5.0 mol.%).

3.8 Surface Topography

Surface texture is the repetitive or unsystematic variation from the nominal surface to forms the three-dimensional topography of the surface. Surface texture include roughness (nano and micro roughness), waviness (macro roughness), lay and flaws. Fig. 13 shows the AFM images of undoped and Sn doped film with different concentrations. Agglomeration of crystallities can be seen in all the films from the AFM images. The estimated average surface roughness of the present samples are 0.015, 0.012 and 0.019 μm for films 0, 10.0 and 20.0 mol.% of Sn concentration. The Fig. 13- (a) are having lower surface roughness and number of voids created. Further, the bumpy surface revealed when the Sn doped level of 10.0 mol.% as shown in Fig. 13-(b). The maximum doping of Sn (20.0 mol.%) the particles are clustered number of places as shown in Fig. 13-(c). These results are correlated with XRD, FESEM and HRTEM results.

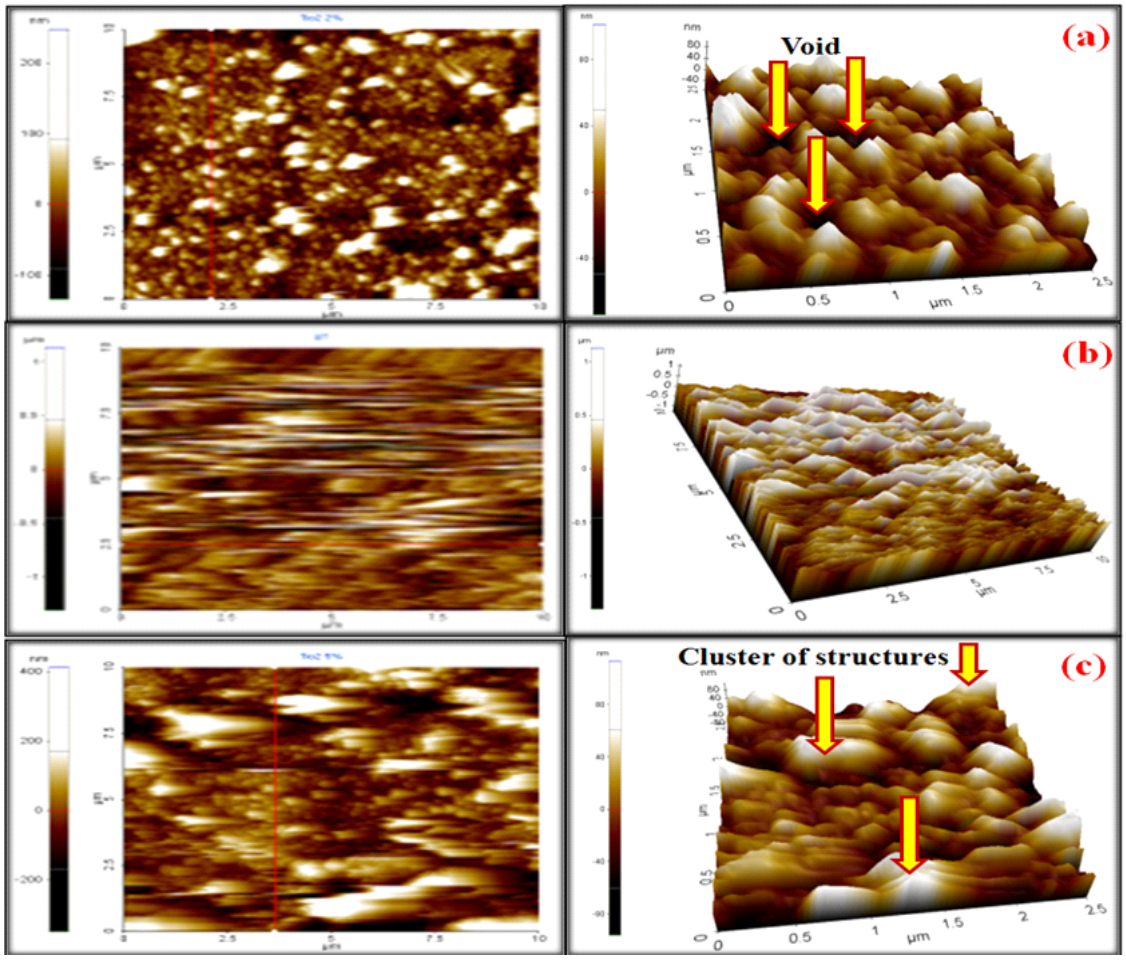

Fig. 13: AFM images of (a) undoped (b) Sn doped with 10.0% and (c) Sn doped with 20.0% of Cu_2O thin films.

4 Conclusions

In this report, a good excellence of undoped and Sn doped cuprous oxide thin films was successively deposited onto glass substrate with the doping steps of 5.0 mol.% using SILAR technique. From X-ray diffraction pattern, closely notice that the Sn doped cuprous oxide film at 10.0 mol.% are high crystalline quality compare than other films. Here, all the films maintain the crystalline orientation peak of (111) plane. The crystallinity of the films varied from 52.07 to 23.24 nm. EDAX analysis indicated that O, Cu and Sn have in the Sn doped film at 10.0 mol.%. Thickness of the film is minimum of Sn doped cuprous oxide film at 10.0 mol.% compare than to other film, and linearly increase the thickness with increases of Sn doing concentration. From the optical studies (UV-vis-NIR and PL), the transmittance of the film increases nearly 70 % and energy band gap values are decreased from 1.70 to 2.18 eV with corresponding doping concentration. A morphological property of the deposited film was investigated by FESEM and HRTEM. It has been establish that the surface morphology and crystalline orientation of the film varying and quality of the film improved for 10.0 mol.% of Sn doping concentration. From AFM analysis, the surface smoothness of the film was determined and the estimated smoothness is 0.015, 0.012 and 0.019 µm. Sn doped with 10.0 mol.% film clearly exhibit bumpy surface compare than to other films. Further investigations such are needs for determined the performance the structural and anticancer activity of the film after annealing a suitable temperature.

References

[1] K. Akimoto, S. Ishizuka, M. Yanagita, Y. Nawa, Goutam K. Paul, T. Sakurai, Thin film deposition of Cu_2O and application for solar cells. *Solar Energy.*,**80**, 715–722, (2006).

[2]AzadehTadjarodi, Omid Akhavan, KeyvanBijanzad, Photocatalytic activity of CuO nanoparticles incorporated in mesoporous structure prepared from bis(2-aminonicotinato) copper(II) microflakes, *Trans. Nonferrous Met. Soc. China.*,**25**, 3634−3642, (2015)

[3] Jinyan Pan, Chengfu Yang, and Yunlong Gao, Investigations of Cuprous Oxide and Cupric Oxide Thin Films by Controlling

the Deposition Atmosphere in the Reactive Sputtering Method, *Sensors and Materials*., **28**, 817–824, (2016).

[4] Kenza Kamli, Zakaria Hadef, Baghdadi Chouial & Bouzid Hadjoudja, Thickness effect on electrical properties of copper oxide thin films, *Surf. Eng*. 2018; DOI: 10.1080/02670844.2018.1475052.

[5] Y. Gulen, F. Bayansal, B. Sahin, H.A. Cetinkara, H.S. Guder, Fabrication and characterization of Mn-doped CuO thin films by the SILAR method, *Ceram. Int.,***39**, 6475–6480, (2013).

[6] C.T. Meneses, J.G.S. Duque, L.G. Vivas, M. Knobel, Synthesis and characterization of TM-doped CuO (TM= Fe, Ni), *J. Non- Cryst. Solids.*,**354**, 4830–4832, (2008).

[7] P. Chand, A. Gaur, A. Kumar, U.K. Gaur, Structural and optical study of Li doped CuO thin films on Si (1 0 0) substrate deposited by pulsed laser deposition , *Appl. Surf. Sci.*,**307**, 280–286, (2014).

[8] D. Barreca, G. Carraro, E. Comini, A. Gasparotto, C. Maccato, C. Sada, G. Sberveglieri, E. Tondello, Novel Synthesis and Gas Sensing Performances of CuO–TiO2 Nanocomposites Functionalized with Au Nanoparticles ,*J. Phys. Chem.*,**C. 115**, 10510–10517, (2011).

[9] Ryan DulaCorpuz and Jason Rayala Albia. Electrophoretic fabrication of ZnO/ZnO-CuO composite for ammonia gas sensing , *Materials Research.*,**17(4)**, 851–856,(2014).

[10] V. Georgieva, M. Ristov, M. Electrodeposited cuprous oxide on indium tin oxide for solar applications , *Sol. Energy Mater. Sol. Cells.*,**73**, 67-73, (2002).

[11] K. Han, M. Tao, Electrochemically deposited p–n homojunction cuprous oxide solar cells , *Sol. Energy Mater. Sol. Cells.* 93, 153-157, (2009).

[12] Negar DasinehKhiavi, Reza Katal, SaeidehKholghiEshkalak , SaeidMasudy-Panah, Seeram Ramakrishna, and Hu Jiangyong, Visible Light Driven Heterojunction Photocatalyst of CuO–Cu_2O Thin Films for Photocatalytic Degradation of Organic Pollutants, *Nanomaterials 2019* : doi: 10.3390/nano9071011

[13] Artur Rydosz. The Use of Copper Oxide Thin Films in Gas-Sensing Applications, *Poland Coatings.*, **8(12)**, 425- 443, (2018).

[14] S.N. Kale, S.B. Ogale, S.R. Shinde, M. Sahasrabuddhe, V. Kulkarni, R. Greene, T. Venkatesan, Magnetism in cobalt-doped thin films without and with Al, V, or Zn codopants *Appl. Phys.* 2003: DOI: 10.1063/1.1564864.

[15] X.P. Gao, J.L. Bao, G.L. Pan, H.Y. Zhu, P.X. Huang, F. Wu,D.Y. Song, Preparation and electrochemical performance of polycrystalline and single crystalline CuO nanorods as anode materials for Li ion battery, *Phys. Chem.* 2004: DOI 10.1021/ip037075k.

[16] P.J.M.Isherwood and J.M.Walls Cupric Oxide-based p-type Transparent Conductors, *Energy Procedia.*, **60**, 129-134, (2014).

[17] A. Dulma , H. Vrielinck, S. Khelifi, DiederikDepla, Sputter deposition of copper oxide films. *Appl. Surf. Sci.*,**492**,711-717, (2019).

[18] Umesh Chandra Binda Raj Kumar DuttaabGurpreet KaurSekhonc Kanhaiya Lal Yadavc J.B.M.Krishnad RanjiniMenoneP.Y.Nabhiraje, implantation induced phase transformation and enhanced crystallinity of as deposited copper oxide thin films by pulsed laser deposition. *Superlattices Microstruct.*, **84**, 24-35, (2015).

[19] Sebastian Eisermann, Achim Kronenberger, Andreas Laufer, Johannes Bieber, Gunther Haas, Stefan Lautenschla¨ ger, Gerd Homm, Peter J. Klar, and Bruno K. Meyer,Copper oxide thin films by chemical vapor deposition: Synthesis, characterization and electrical properties, *Phys. Status Solidi A*,**209**:531–536, (2012).

[20] Hassan ZareAsla, Seyed Mohammad Rozatia , Spray Deposited Nanostructured CuO Thin Films: Influence of Substrate Temperature and Annealing Process, *Materials Research.* 2018: DOI: http://dx.doi.org/10.1590/1980-5373-MR-2017-0754.

[21] K. Santra, C. K. Sarkar, M. K. Mukherjee and B. Ghosh, Copper oxide thin films grown by plasma evaporation method, *Thin Solid Films.*,**213**, 226-229, (1992).

[22] V. Dhanasekaran T. Mahalingam , R. Chandramohan , Jin-Koo Rhee , J.P. Chu, Electrochemical deposition and characterization of cupric oxide thin films, *Thin Solid Films.*, **520**, 6608-6613 (2012).

[23] A. Vasuhi, R. John Xavier, R. Chandramohan, S. Muthukumaran, K. Dhanabalan, M. Ashokkumar & P. Parameswaran, Effect of heat-treatment on the structural and optical properties of Cu_2S thin films deposited by CBD method, *J Mater Sci: Mater Electron.* 2014: DOI 10.1007/s10854-013-1652-x

[24] Akinobu Yamaguchi, Ikuo Okada, Takao Fukuoka, Mari Ishihara, Ikuya Sakurai, and Yuichi Utsumi, One-Step Synthesis of Copper and Cupric Oxide Particles from the Liquid Phase by X-Ray Radiolysis Using Synchrotron Radiation, *J. Nanomater.* 2016: http://dx.doi.org/10.1155/2016/8584304.

[25] Senthuran Karthick Kumar, Sepperumal Murugesan, Santhanakrishnan Suresh, and Samuel Paul Raj, Nanostructured CuO Thin Films Prepared through Sputtering for Solar Selective Absorbers, *J. Sol. Energy.* 2013: http://dx.doi.org/10.1155/2013/147270.

[26] Felipe Cemin, Daniel Lundin, Clarisse Furgeaud, Anny Michel, Guillaume Amiard, Tiberiu Minea & Gregory Abadias , Epitaxial growth of Cu(001) thin films onto Si(001) using a single-step HiPIMS process, *Scientific Reports,* **7**, 1655-1664, (2017).

[27] A. T. Ravichandran, K. Dhanabalan, A. Vasuhi, R. Chandramohan, and Srinivas Mantha, Morphology, Bandgap, and Grain Size Tailoring in Cu_2O Thin Film by SILAR Method, *IEEE Trans Nanotechnol*, **14**, 108-112 (2015).

[28] E.F. Keskenler, G.Turgut, S. Aydin, S. Dogan, and B.B. Duzgun, The Effect of Fluorine and Tungsten Co-Doping on Optical, Electrical and Structural Properties of Tin (IV) Oxide Thin Films Prepared by Sol-Gel Spin Coating Method, *Optica Applicata*.,**4**, 663-677, (2013).

[29] A.T. Ravichandran, K.Dhanabalan, S. Valanarasu, A. Vasuhi & A. Kathalingam, Role of immersion time on the properties of SILAR deposited CuO thin films, *J Mater Sci: Mater Electron*, **26 (2)**, 921-926, (2015).

[30] S. Satheeskumar, S. Vadivel, K.Dhanabalan, A. Vasuhi, A. T. Ravichandran, K. Ravichandran, Enhancing the structural,

optical and magnetic properties of Cu_2O films deposited using a SILAR technique through Fe-doping, *J Mater Sci: Mater Electron.* **29 (11)**, 9354-9360, (2018).

[31] P.-H. Hsieh, Y.-M. Lu, W.-S. Hwang, J.-J. Yeh, W.-L. Jang, Effect of Al content on electrical conductivity and transparency of P-type Cu-Al-O thin film., *Surf. Coat*. DOI:10.1016/j.surfcoat.2010.07.077.

[32] K. Dhanabalan, A. T. Ravichandran, K. Ravichandran, S. Valanarasu, Srinivas Mantha, Effect of Co doped material on the structural, optical and magnetic properties of Cu_2O thin films by SILAR technique, *J Mater Sci: Mater Electron*., **28 (5)**, 4431-4439, (2017).

[33] Nuengruethai Ekthammathat, TitipunThongtem, Somchai Thongtem. Antimicrobial activities of CuO films deposited on Cu foils by solution chemistry, *Appl. Surf. Sci*.,**277**, 211-217, (2013).

[34] T. Van Tran, S. Turrell, M. Eddafi, B. Capoen, M. Bouazaoui, P. Roussel, S. Berneschi, G. Righini, M. Ferrari, S.N.B. Bhaktha, O. Cristini, and C. Kinowski, Investigations of the Effects of the Growth of SnO_2 Nanoparticles on the Structural Properties of Glass-Ceramic Planar Waveguides Using Raman and FTIR Spectroscopies. *J. Mol. Struct.,***976** , 314-319, (2010).

[35] A. T. Ravichandran, K. Dhanabalan, K. Ravichandran, R. Mohan, K.Karthika, A. Vasuhi, B. Muralidharan, Tuning the Structural and Optical Properties of SILAR-Deposited Cu_2O Films Through Zn Doping, *Acta Metall. Sin. (Engl. Lett.),* **28 (8)**, 1041-1046, (2015).

[36] Ali Rahmati, Ali BalouchSirgani, Mehdi Molaei& Masoud Karimipour. Cu-doped ZnO nanoparticles synthesized by simple co-precipitation route. *Eur. Phys. J. Plus*, **129,** 250-256, (2014).

[37] Srinivas Mantha, A.T. Ravichandran, K. Dhanabalan, Vasuhi Dhanabalan, and R. Chanramohan, *Morphology, bandgap and grain size tailoring in Cu_2O thin film by modified chemical bath deposition technique and methods employed thereof*, Intellectual Property India, 321095, Sep.23, (2019).

[38] K. Maaz , A. Mumtaz, S.K. Hasanian, A. Ceylan, Synthesis and magnetic properties of cobalt ferrite ($CoFe_2O4$) nanoparticles prepared by wet chemical route,. *J. Magn. Magn. Mater.*, **308**, 289 –295, (2007).